

METHANE BUDGET OF A LARGE GAS HYDRATE PROVINCE OFFSHORE GEORGIA, BLACK SEA

Matthias Haeckel*

Anja Reitz

Ingo Klaucke

Leibniz Institute of Marine Sciences (IFM-GEOMAR)

Wischofstr. 1-3, D-24148 Kiel

Germany

ABSTRACT

The Batumi Seep Area, offshore Georgia, Black Sea, has been intensively cored (gravity cores and TV-guided multi-cores) to investigate the methane turnover in the surface sediments. The seep area is characterized by vigorous methane gas bubble emanations. Geochemical analyses show a microbial origin of the methane and a shallow fluid source. Anaerobic methane oxidation rapidly consumes the SO_4^{2-} within the top 5-20 cm, but significant upward fluid advection is not indicated by the porewater profiles. Hence, the Batumi Seep Area must be dominated by methane gas seepage in order to explain the required CH_4 flux from below. 1-D transport-reaction modelling constrains the methane flux needed to support the observed SO_4^{2-} flux as well as the rate of near-surface hydrate formation. The model results correlate well with the hydro-acoustic backscatter intensities recorded and mapped bubble release sites using the sonar of a ROV.

Keywords: methane turnover, gas hydrates, gas seepage, cold vents, geochemistry, numerical modeling, anaerobic methane oxidation, Black Sea

NOMENCLATURE

$[C]$ concentration of the dissolved constituent [mmol dm^{-3}]

D_i diffusion coefficient of the dissolved constituent i [$\text{cm}^2 \text{a}^{-1}$]

GH porosity reduction due to gas hydrate formation [(volume gas hydrate) (volume wet sediment) $^{-1}$]

d_{bubble} diameter of a gas bubble [cm]

f_{bubble} frequency of gas bubble ebullition [bubbles a^{-1}]

F_{CH_4} methane gas flow [$\text{dm}^3 \text{a}^{-1}$]

g acceleration through gravity [= 9.81 g cm^{-3}]

k_{AOM} rate constant of anaerobic methane oxidation (AOM) [$\text{dm}^3 \text{mmol}^{-1} \text{a}^{-1}$]

K_{eddy} mixing coefficient for eddy diffusivity [$\text{cm}^2 \text{a}^{-1}$]

k_{GH} kinetic constant of gas hydrate formation [(volume gas hydrate) (volume wet sediment) $^{-1} \text{a}^{-1}$]

k_{MB} kinetic constant of methane gas bubble dissolution [a^{-1}]

L_{MB} methane concentration in equilibrium with the gas phase [mmol dm^{-3}]

L_{GH} equilibrium concentration of methane in the presence of a methane hydrate phase [mmol dm^{-3}]

M_{GH} molar weight of natural gas hydrate [g mol^{-1}]

r_{bubble} radius of a gas bubble [cm]

n_{bubble} number of gas bubbles in bubble tube

R_i rate of biogeochemical reaction i [$\text{mmol dm}^{-3} \text{a}^{-1}$]

t time [a]

t_{rise} rise time of gas bubble through sediment [a]

u advection velocity [cm a^{-1}]

u_0 advection velocity at the sediment surface [cm a^{-1}]

u_{rise} rise velocity of gas bubble [cm a^{-1}]

V_{bubble} average volume of a gas bubble in the sediment [$\text{dm}^3 \text{a}^{-1}$]

w sediment burial velocity [cm a^{-1}]

w_{∞} sediment burial velocity at infinite depth [cm a^{-1}]

x depth [cm]

z diffusive sublayer around gas bubble [cm]

* Corresponding author: Phone: +49 431 600 2123 Fax +49 431 600 2928 E-mail: mhaeckel@ifm-geomar.de

β attenuation coefficient for the exponential decrease of porosity with depth [cm^{-1}]

f porosity [(volume porewater) (volume wet sediment) $^{-1}$]

f_{∞} porosity at infinite depth

f_0 porosity at the sediment surface

q^2 tortuosity

r_{GH} density of methane hydrate [g cm^3]

r_{PW} density of sea water [g cm^3]

INTRODUCTION

Methane seepage makes up an important part of the global carbon cycle as it contributes methane to the biosphere, hydrosphere and atmosphere. Seabed seepage comprises the flow of gases and natural fluids, from rocks and sediments, through the seabed into the water column; preferably along faults or comparable conduits where migration is focused. Methane seepage occurs in every sea and ocean in various plate tectonic and oceanographic settings [e.g., 1]. In marine sediments, methane is the most common hydrocarbon and its potential sources are organic matter buried in marine sediments and (i) decomposed by microbial activity (microbial) or (ii) degraded by thermocatalytic processes (thermogenic), or (iii) the methane is produced as a result of degassing of mafic magmas and/or cooling of igneous mafic rocks (abiogenic).

How significant is methane seepage for the biosphere, hydrosphere and atmosphere. The main effect on the biosphere is the support of so called 'cold seep communities' [e.g., 2] by methane and the production of hydrogen sulfide. Hydrogen sulfide is generated in the subsurface sediments due to the anaerobic oxidation of methane (AOM) by consortia of microbes and subsequently utilized by sulfide-oxidizing microbes (e.g., *Beggiatoa* sp.) [3]. A by-product of AOM is the precipitation of methane-derived authigenic carbonates. Generally, most of the methane migrating to the seabed is consumed by AOM [4]. However, where seepage is focused the flux rate might exceed its utilization rate allowing methane to seep through the sediment surface into the hydrosphere; either as gentle seepage or as catastrophic gas escapes.

Even though all methane seeps might affect the biosphere and hydrosphere, deep water seeps (>100 m) are unlikely to contribute to the atmosphere as gas bubbles lose methane to the water as they rise [5, 6]. Only catastrophic events may aid methane to pass rapidly through the water

into the atmosphere [e.g., 7]. Leifer and Patro [8] summarized that the fraction of methane seeping through the seabed and rising through the water column to reach the atmosphere are primarily constrained by the water depth, and the temperature, salinity, and methane concentration of the water, and the initial bubble size. However, methane that did not reach the atmosphere might relevantly contribute to the hydrosphere.

As the CH_4 concentrations of the Black Sea's water column is in steady-state [9] it must be assumed that the source is balanced by the sink of CH_4 . Supposing this steady-state Reeburgh et al. [10] estimated an average methane flux of $1.5 \text{ mol m}^{-2} \text{ a}^{-1}$ from the sediments between 100 and 1500 m water depth to the water column to balance the methane sinks. However, on the basis of a shelf core they determined a methane flux of only $0.2 \text{ mol m}^{-2} \text{ a}^{-1}$. Furthermore, it has been shown that diffusive methane contribution from the sediments is rather small [e.g., 11]. Reeburgh et al. [12] suggest that the decomposition of methane gas hydrates might account as an additional methane source balancing the methane budget. Recently, other geochemists [7, 9, 13, 14] postulate that methane emanating from seeps must be an important requirement in the methane budget. The methane radiocarbon investigation of Kessler et al. [9] indicate that seeps and decomposing hydrates emit between 3.60 to 5.65 Tg a^{-1} of CH_4 to the Black Sea water column and the escape to the atmosphere amounts to 0.05 to 0.21 Tg a^{-1} .

Here, we present geochemical data and results from numerical transport-reaction simulations of sediments from the Batumi Seep area offshore Georgia. Vigorous fluid and gas seepage was identified by hydro-acoustic anomalies in the water column and by areas of high backscatter intensity [15] (Fig. 1). By combining these information with the geochemical investigations we calculate a methane budget of the Batumi Seep area, which assigns a step towards a better deciphering the importance of cold seeps and mud volcanoes to the methane budget of the Black Sea.

SITE DESCRIPTION

The Batumi Seep (Fig. 1), covering an area of 0.5 km^2 , is located in about 850 m water depth on the Kobuleti Ridge [15]. The Kobuleti Ridge is part of a complex system of W-E striking canyon and ridge structures within the offshore extension of the Rioni Basin off Georgia [15, 16]. The Rioni Basin developed as one of two foreland basins

between the Greater Caucasus Thrust Belt (North) and the Adjara-Trialet Thrust Belt as part of the eastern Pontides (South) [15].

The Batumi Seep area comprises subsurface authigenic carbonate precipitations and gas hydrates and is actively emitting methane gas into the water column, which is evident by hydro-acoustic reflections of the gas bubbles (commonly called: gas flares). These gas flares coincide with high seafloor backscatter intensity and characterize the central part of the seep area [15]. Areas of medium backscatter intensity surround the central part and show a sharp contact to the background sediments (Fig. 1).

The Batumi seep, as well as the other seeps offshore Georgia, are different from other cold seeps observed so far in the Black Sea as it is located within the thermodynamic stability zone of methane hydrates (upper limit around 725 m water depth based on 9 °C bottom water temperature; [15, 16]) and it does not show indication for mud flow. The two types of cold seeps, generally observed in the Black Sea, are shallow fluid and gas emission from the lower gas hydrate stability zone [e.g., 17, 18] and deep-water mud volcanoes [e.g., 19].

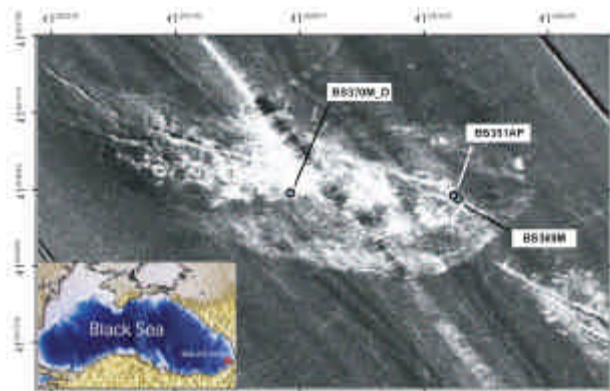


Figure 1: Backscatter map of the Batumi Seep area (modified after [15]) indicating the coring locations. White color corresponds to high backscatter and dark to low backscatter intensities. Inlet: Overview map of the Black Sea indicating the location of the Batumi Seep area.

METHODS

Sediment sampling

During the TTR-15 expedition (UNESCO Training Through Research Program) with RV Professor Logachev in June 2005, as part of the German collaborative research project METRO

(<http://www.marum.de/METRO.html>), sediments were collected with a gravity corer (GC), a video-guides multi-corer (MC), and a dynamic autoclave piston corer (DAPC; [20]) at a water depth of about 850 m (Table 1). To enable rapid sampling immediately after core retrieval, the inner tube of the gravity corer was lined with a tubular plastic bag. Sediments were sampled in 5-40 cm resolution directly on deck and subsequently transferred into the cold room (4-8 °C) for further treatment under in-situ temperature (~9 °C [12]). The MC cores were directly transferred into the cold room and sampled in 0.5-2 cm resolution. Pore fluids were extracted using a low pressure filtration system (0.2 µm regenerated cellulose Nuclepore filters) at pressures of up to 5 bar. From each wet sediment slice about 5 ml were collected for porosity analyses. Porosity was determined in the shore-based laboratory at IFM-GEOMAR as volume of porewater per volume of wet sediment by weight difference before and after freeze-drying assuming a dry sediment density of 2.5 g/cm³ and a porewater density of 1.021 g/cm³.

Pore fluid analyses

Porewater sulfide (HS⁻), total alkalinity (TA) and chloride (Cl⁻) concentrations were measured onboard, whereas the dissolved sulfate (SO₄²⁻) content was analyzed in the shore-based laboratory at IFM-GEOMAR using ion chromatography. HS⁻ was determined as methylene blue [21] using a Hitachi UV/VIS spectrophotometer. TA was measured by titration with 0.02N HCl using the Tashiro indicator (a mixture of methyl red and methylene blue) and stripping any CO₂ and H₂S produced during the titration by bubbling the solution with argon. The Cl⁻ content was determined by titration after Mohr with 0.1M AgNO₃ solution using a mixture of potassium chromate/dichromate as indicator. Both titration methods were calibrated with the IAPSO seawater standard.

Model description

A numerical transport-reaction model was developed according to [22, 23] to simulate the observed porewater data and to determine rates of upward fluid flow, methane emission, gas hydrate formation, and AOM. The model considers five chemical species, chloride, methane, sulfate, hydrogen sulfide, total alkalinity (simplified as sum of HCO₃⁻ and HS⁻), and gas hydrate as well as the porosity change due to gas hydrate formation.

The well-known partial differential equations for early diagenesis [24] were applied:

a) Solutes (i.e. for Cl^- , CH_4 , SO_4^{2-} , HS^-):

$$\frac{\partial \mathbf{f}[C]}{\partial t} = \frac{\partial}{\partial x} \left(\mathbf{f} \frac{D_i}{q^2} \frac{\partial [C]}{\partial x} - \mathbf{f} u [C] \right) + \sum R_i \quad (1)$$

b) Solids (i.e. for pore-filling methane hydrate):

$$\frac{\partial GH}{\partial t} = -\mathbf{f} w \frac{\partial GH}{\partial x} + \sum R_i \quad (2)$$

Generally, the porosity depth distribution, $\mathbf{f}(x)$, does not change significantly with time and can thus be prescribed by an empirical function fitted to the measured data. However, porosity is reduced if gas hydrates are formed in the pore space of the sediment. Consequently, porosity was calculated as a function of time and depth:

$$\mathbf{f}(x, t) = \mathbf{f}_\infty + (\mathbf{f}_0 - \mathbf{f}_\infty) e^{-bx} - GH(x, t) \quad (3)$$

Assuming steady state compaction, the sediment burial velocity can be expressed as:

$$w(x, t) = \frac{1 - \mathbf{f}_\infty}{1 - \mathbf{f}(x, t)} w_\infty \quad (4)$$

Since burial and compaction at cold vent sites are much smaller than the upward fluid flow, they can be neglected and the porewater advection velocity is:

$$u(x, t) = \frac{\mathbf{f}_0}{\mathbf{f}(x, t)} u_0 \quad (5)$$

The molecular diffusion coefficient was corrected for salinity, temperature, and pressure according to [25] and the Stokes-Einstein relation. Finally, the molecular diffusion coefficient was also corrected for tortuosity using the expression $1-2\ln\mathbf{f}$ [26].

Methane hydrate formation is assumed proportional to the saturation state of methane in the porewater with respect to its equilibrium concentration in the presence of the hydrate phase (L_{GH}):

$$R_{GH} = k_{GH} \left(\frac{\text{CH}_4}{L_{GH}} - 1 \right) \quad (6)$$

L_{GH} was calculated following [27].

Since hydrate formation withdraws methane from the porewater, the rate of methane consumption (in units of mole CH_4 per volume porewater and time) is related to R_{GH} by:

$$R_M = \frac{\mathbf{r}_{GH}}{M_{GH} \mathbf{f}} R_{GH} \quad (7)$$

As gas bubbles rise through the sediments they are replenishing the porewater methane content. A first order rate accounts for this dissolution:

$$R_{MB} = k_{MB} (L_{MB} - \text{CH}_4) \quad (8)$$

The methane concentration in equilibrium with the gas phase, L_{MB} , is calculated following [27].

Parameter	Value
<i>Fixed:</i>	
Maximum depth of calculation	500 cm
simulation time	500 a
Temperature	9.0 °C
Pressure	85.5 atm
w_∞	0.02 cm/a ^a
ϕ_0	0.89(7) ^b
ϕ_∞	0.71(4) ^b
β	0.018(9) cm ^{-1b}
$[\text{Cl}^-](x=0, t)$	350 mM
$[\text{Cl}^-](x=500\text{cm}, t)$	250 mM
$[\text{CH}_4](x=0, t)$	0.001 mM
$[\text{CH}_4](x=500\text{cm}, t)$	L_{MB}
$[\text{SO}_4^{2-}](x=0, t)$	18 mM
$[\text{SO}_4^{2-}](x=500\text{cm}, t)$	0 mM
$[\text{HS}^-](x=0, t)$	0 mM
$[\text{HS}^-](x=500\text{cm}, t)$	0 mM
$[\text{HCO}_3^-](x=0, t)$	5 mM
$[\text{HCO}_3^-](x=500\text{cm}, t)$	13 mM
$\text{GH}(x=0, t)$	0 %pv
$d\text{GH}/dx _{x=500\text{cm}, t}$	0
L_{GH}	93 mM ^c
L_{MB}	107.7 mM ^c
M_{GH}	122.3 g/mol ^d
ρ_{GH}	0.9 g/cm ^{3 e}
ρ_{PW}	1.021 g/cm ^{3 f}
<i>Adjusted:</i>	
u_0	0.5 cm/a
k_{GH}	0.005 a ⁻¹
k_{MB}	0.3 a ⁻¹
k_{AOM}	0.8 mM ⁻¹ a ⁻¹

(a) [28]

(b) results of least-squares porosity fit ($\chi^2 = 0.02$); 2σ standard deviation given in brackets in terms of last digit

(c) calculated following [27]

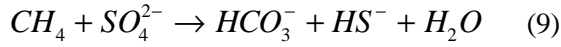
(d) [29]

(e) [30]

(f) calculated following [31] based on the mean Cl^- concentration

Table 1. Parameters and boundary conditions used in the numerical model.

As additional reaction affecting dissolved methane concentrations, anaerobic methane oxidation (AOM) was included:



Mathematically, a second-order rate law describes this redox reaction:

$$R_{AMO} = k_{AMO} [CH_4] [SO_4^{2-}] \quad (10)$$

During methane hydrate formation chloride is excluded from the hydrate phase and added to the surrounding porewater. The rate of chloride exclusion, R_{Cl} , is related to the rate of hydrate formation, $R_{GH} = dGH/dt$ by [23]:

$$R_{Cl} = \frac{dCl}{dt} = \frac{Cl r_{GH}}{r_{PW} \mathbf{f} - r_{GH} dGH} R_{GH} \approx Cl \frac{r_{GH}}{r_{PW} \mathbf{f}} R_{GH} \quad (11)$$

where the simplification holds when $r_{GH} \cdot dGH \ll r_{PW} \mathbf{f}$ for small dt .

The spatial derivatives of the partial differential equations (PDEs) were approximated with central finite differences. The resulting system of ordinary differential equations (ODEs) was solved using the NDSolve object of Mathematica[®] applying the method-of-lines technique. Initial conditions are based on the steady state profiles of a reference core (dashed lines in Fig. 2). Upper and lower boundary conditions as well as fixed and adjusted model parameters are given in Table 1.

RESULTS AND DISCUSSION

Modelling results

A sensitivity analyses was performed to constrain the values of these five fit parameters. The best fit (Fig. 2) to the observed data was achieved for low fluid advection velocities ($u_0 = 0.5$ cm/a) as the measured chloride profile does not show significant curvature, except for the hydrate related anomaly. The rate constant for anaerobic methane oxidation (k_{AOM}) basically influences the increase in sedimentary hydrate content near the surface because AOM competes with hydrate formation for the available dissolved methane. A minimum AOM rate constant of $k_{AOM} = 0.8$ mM⁻¹ a⁻¹ is able to fit the observed sulfate data and also resemble the steep increase in hydrate concentration as it can be inferred from the measured Cl⁻ anomaly in core BS351AP (Fig. 2). Diffusion of methane from below is only able to form a few vol% of hydrate (i.e., volume of gas hydrate per volume of wet sediment). In order to build up considerable amounts of hydrate (i.e., >10 vol%) an additional

methane source is needed. Therefore, methane gas bubble dissolution has been included in the model. This process is also required in order to deliver enough methane to the surface sediments, so that the onset of hydrate formation at a sediment depth of ~65 cm can be resembled (see start of observed Cl⁻ anomaly). The predicted rate constant for methane gas bubble dissolution is $k_{MB} = 0.3$ a⁻¹. To balance this increased methane flux to the porewater and keep dissolved methane concentrations at equilibrium with the hydrate phase ($L_{GH} = 93$ mM; Tab. 1), hydrate formation needs to proceed with a rate constant of $k_{GH} = 0.05$ a⁻¹. Finally, a simulation time of several hundreds of years (i.e., here 500 a) ensures that the modeled solute concentrations (Cl⁻, CH₄, SO₄²⁻, HS⁻, and HCO₃⁻) are at steady state; the solid gas hydrate profile, of course, is not at steady state after this time. For a simulation time of 500 years, the model predicts an average hydrate concentration of ~12 vol%. This corresponds to the amount calculated directly from the observed chloride anomaly (i.e., ~11 vol%). However, it is difficult to conclude an age of the Batumi Seep area from this finding, because hydrate related seeps are dynamic systems and methane fluxes can vary over time by orders of magnitude. In contrast, the model simulation assumes a constant methane flux and a constant hydrate formation rate over the entire simulation time.

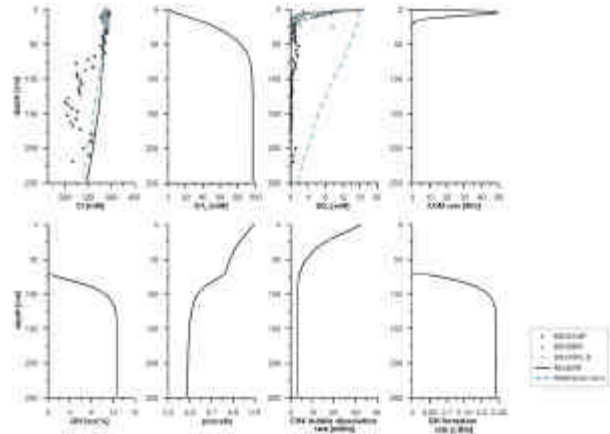


Figure 2: Result of the numerical 1-D transport-reaction model of hydrate formation in the Batumi Seep Area (solid lines). The values of the adjusted model parameters of this simulation are given in Table 1. Dots represent the measured data at the seep, whereas dashed lines refer to the observed reference situation.

Methane flux budget

The purpose of this section is to connect the calculated methane sinks (i.e., benthic flux, AOM and hydrate formation) and sources (i.e., gas dissolution rate) to the gas bubble motion through the surface sediments and attempt to calculate a representative methane flux for the entire Batumi Seep area.

From the numerical model results a benthic methane flux into the overlying water column of $7.9 \text{ mol/m}^2/\text{a}$ is calculated from the concentration gradient at the sediment surface. About a factor of 2 lower is the consumption through anaerobic oxidation of methane (AOM) (i.e., $3.7 \text{ mol/m}^2/\text{a}$) that is due to reaction with sulfate diffusing into the sediment from the overlying water column.

The simulated hydrate formation represents a sink for methane from the dissolved and gas phase. This is particularly true for seep systems with considerable amounts of near-surface hydrates ($>1\text{-}3 \text{ vol}\%$), as we have found in the Batumi Seep area. The modeled and observed concentrations of gas hydrates of $11\text{-}12 \text{ vol}\%$ correspond to $0.81\text{-}0.88 \text{ mol}$ of hydrate per liter of bulk sediment, which is equivalent to $0.61\text{-}0.66 \text{ mol/l}$ of dissolved CH_4 . The numerical model calculates a depth-integrated rate of $7.1 \text{ mol/m}^2/\text{a}$ to match these concentrations.

Haeckel et al. [23] derived an equation that relates the methane gas bubble dissolution rate to the number of gas bubbles present in the sediment:

$$k_{MB} = \frac{4pf r_{bubble}^2 D_{CH_4}}{z} n_{bubble} \quad (12)$$

According to this equation, the bubble dissolution rate derived from the numerical transport-reaction modelling corresponds to $0.13 \text{ gas bubbles per dm}^3$ of sediment ($r_{bubble} = 1 \text{ mm}$, assuming a diffusive sublayer of $z = 0.1 \text{ mm}$ around the bubble). Under in situ pressure and temperature conditions this is equivalent to an amount of $\sim 1.9 \text{ mM}$ of methane gas. The numerical simulation predicts a methane flux from the gas phase to the dissolved phase of $17.5 \text{ mol/m}^2/\text{a}$.

Finally, the model predicts that overall about 93 % of the methane demanded by the sinks is provided from methane gas bubble transport and only a minor fraction of 7 % contributes from methane solute transport (i.e., diffusion and advection).

Gas bubble rise in surface sediments

Gas bubbles rising through surface sediments have been widely observed and investigated in coastal

sediments [32-37]. In these sediments, apparent diffusivities 2-3 times higher than molecular diffusion have been determined for dissolved constituents. Furthermore, recent studies [38, 39] have shown that gas bubbles ascend through soft sediments by crack formation and propagation.

In addition, porewater profiles with a bottom-water signature, present in sediment to depths of several meters, have repeatedly been reported in the literature [e.g., 40, 41]. Commonly, these profiles have been explained by meter-scale bioirrigation of unknown macrofauna, but Fossing et al. [42] also mention the possibility of methane ebullition. In the respective studies, these types of porewater distributions are found in organic-rich sediments at continental margins and other high-productivity areas, such as the Congo Fan and the Amazon Shelf, as well as in upwelling regions, such as the South Atlantic off Namibia. In a previous study [43] similar observations have been observed, reaching down as far as 3 m into the sediment, in the organic-rich sediments northeast off Sakhalin Island in the Sea of Okhotsk.

While bioirrigation has been shown to occur in the top few decimetres of the sediment [e.g., 44, 45-47], we propose that irrigation caused by rising gas bubbles is more likely to explain such observations on a meter scale [43]. Methane gas bubbles produced by methanogenesis or methane hydrate dissociation rise through the sediment, thereby, mixing the porewater and ultimately mixing bottom-water concentrations down into the sediment. The wake of a rising gas bubble leads to turbulent mixing of porewater (Fig. 3). Eddy diffusivities orders of magnitude larger than molecular diffusion can be assigned to this process (Fig. 4; [43]).

This mechanistic explanation of gas bubble transport in surface sediments and induced porewater irrigation is underpinned by the presented geochemical data and numerical analysis of the Batumi Seep area. For the irrigation-like porewater profiles found here, bioirrigation can be excluded as a possible explanation because the Batumi seep area is located in water depths of 850 m, where the water mass of the Black Sea is completely anoxic (oxic-anoxic boundary is $\sim 150 \text{ m}$ below the sea surface) and does not allow for macro- or meiofauna life in this environment.

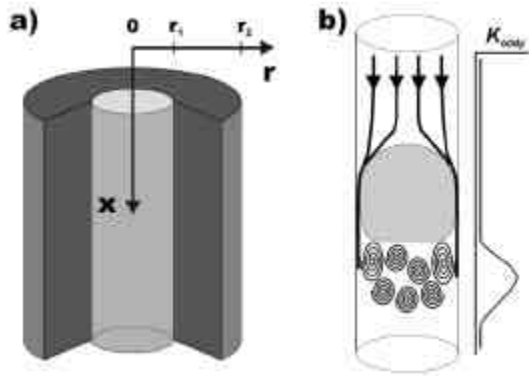


Figure 3: (a) Simplified cylindrical geometry of a gas bubble tube in the sediment. It consists of 2 domains, representing the gas bubble tube (light grey) of radius r_1 and the surrounding sediment (dark grey). The spacing between adjacent tubes is $2(r_2-r_1)$. (b) Schematic sketch of a single bubble rising in a tube. Streamlines indicate flow of water relative to bubble; vortices indicate turbulence in the wake of the bubble. The attached graph sketches the depth distribution of the corresponding eddy diffusion coefficient.

Finally, we derive a relation between eddy diffusive porewater mixing and methane gas flux. This provides us with a measure of the gas flux in the sediments that is otherwise difficult to obtain since the general diagenetic equation (Eq. 1) does only govern the dissolved methane flux and the bubble dissolution rate gives only the gas fraction transferred to the aqueous phase. This fraction is generally low because the interaction time of a rising gas bubble with the surface porewater is usually very short (see discussion below).

Davies and Taylor [48] have shown that gas bubbles, which ascend through a pipe filled with water, reach a terminal rise velocity, u_{rise} , proportional to the bubble radius, r_{bubble} . Furthermore, Prandtl and Tietjens [49] state that an eddy diffusion coefficient (K_{eddy}) for turbulent mixing is proportional to the velocity of the wave (v) times its mixing length (d), i.e., $K_{eddy} \propto vd$. A gas bubble rising in a tube completely mixes a volume of water equivalent to its own volume at any time (Fig. 4b). Hence, the mixing length is equivalent to the diameter of the bubble, d_{bubble} , and we yield the means to relate the eddy diffusion coefficient to bubble rise velocities and the tube geometry:

$$K_{eddy} \approx u_{rise} \cdot d_{bubble} = 0.928 \sqrt{g \cdot r_{bubble}^3} \quad (13)$$

This equation gives a theoretical maximum for the eddy diffusion coefficient.

Since the rise velocity, u_{rise} , provides us with the total time of rise, t_{rise} , for a given tube length and continuous bubble streams require a certain amount of bubbles, n_{bubble} , with diameter, d_{bubble} , in the tube, equation 13 can be written as:

$$K_{eddy} \approx u_{rise} \cdot d_{bubble} = d_{bubble}^2 \frac{n_{bubble}}{t_{rise}} \quad (14)$$

Figure 4b displays a semi-logarithmic plot of K_{eddy} as a function of the bubble frequency (i.e., $f_{bubble} = n_{bubble}/t_{rise}$). Finally, the bubble frequency can easily be translated into a methane flow by multiplying with the average volume of a gas bubble, V_{bubble} :

$$F_{CH_4} = f_{bubble} \cdot V_{bubble} = \frac{K_{eddy}}{4r_{bubble}^2} V_{bubble} \quad (15)$$

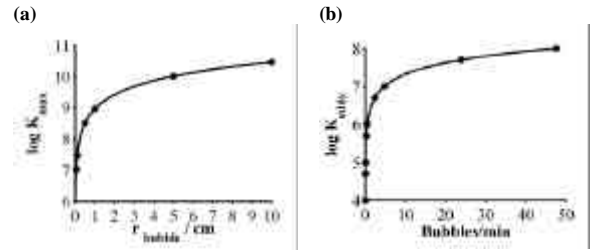


Figure 4: Eddy diffusion coefficient as a function of (a) bubble radius (Eq.13) and (b) bubble frequency (Eq. 14 and a bubble radius of 1 cm). Dots represent parameter values used in the 3-D model realizations of Haeckel et al. [43].

Haeckel et al. [43] have shown that eddy diffusivities need to be at least 2-3 orders of magnitude larger than molecular diffusion (i.e., $K_{eddy} > 10^5 \text{ cm}^2/\text{a}$) to visibly affect the porewater profiles. This mixing coefficient translates into a methane gas flux of 10^3 - $10^6 \text{ mol}/\text{m}^2/\text{a}$ (depending on other parameters, such as bubble tube density and tube geometry) [43]. Hence, the estimated gas flux is much larger than the modelled dissolved methane fluxes as expected from the short interaction time of the gas bubble during its ascent through the surface sediment.

CONCLUSIONS

On one hand, from our numerical analyses we were able to derive a well-constrained dissolved methane flux of about $7.9 \text{ mol m}^{-2} \text{ a}^{-1}$ into the Black Sea water body (i.e., $2.45 \cdot 10^6 \text{ mol}/\text{a}$ over the entire area of the Batumi Seep of 0.31 km^2). This

value compares well to average spatial methane fluxes from cold seeps related to active hydrate formation, such as Hydrate Ridge at the Cascadia margin (i.e., 24 mol m⁻² a⁻¹ over an area of 0.4 km² [50]).

On the other hand, we were able to gain an independent, but rough estimate of the methane gas flux through the surface sediments from our conceptual model of bubble-induced porewater mixing that corresponds well with the calculated methane demand from hydrate formation. This methane gas flux of 10³-10⁶ mol m⁻² a⁻¹ lies well within the range of focussed methane seepage rates reported (i) from Hydrate Ridge for methane hydrate formation (i.e., 10³-10⁴ mol m⁻² a⁻¹) [23], (ii) for discrete methane discharge at Hydrate Ridge (i.e., 4·10⁵ mol m⁻² a⁻¹) [51], and (iii) gas seepage at the Coal Oil Point gas seep (i.e., 8·10⁷ mol m⁻² a⁻¹) [52].

In a next step, we will apply a geographical information system (GIS) to quantitatively combine the calculated methane fluxes with spatial information on seepage activity from the hydro-acoustic backscatter map and the bubble release sites mapped during ROV deployments in the Batumi Seep area. This will further improve our spatial methane flux and its relevance to the Black Sea methane budget.

ACKNOWLEDGEMENTS

We would like to thank B. Domeyer, K. Nass, R. Surberg, A. Bleyer, M. Bausch, and M. Reuschel for support and geochemical analyses during and after the TTR-15 expedition. We also greatly appreciate the support by the masters and crew of RV Logachev and the TTR-15 scientific party. Financial support was granted by the German-Russian WTZ cooperation and the German BMBF-Geotechnologien projects METRO (03G0604A) and COMET (03G0600D).

REFERENCES

- [1] Judd AG. *The global importance and context of methane escape from the seabed*. *Geo-Marine Letters* 2003;23:147-154.
- [2] Sibuet M, Olu K. *Biogeography, biodiversity and fluid dependence of deep-sea cold-seep communities at active and passive margins*. *Deep-Sea Research I* 1998;45:517-567.
- [3] Boetius A, Ravensschlag K, Schubert CJ, Rickert D, Widdel F, Gieseke A, Amann R, Jørgensen BB, Witte U, Pfannkuche O. *A marine microbial consortium apparently mediating anaerobic oxidation of methane*. *Nature* 2000;407:623-626.
- [4] Reeburgh WS, Heggie DT. *Microbial methane consumption reactions and their effect on methane distributions in freshwater and marine environments*. *Limnology and Oceanography* 1977;22(1):1-9.
- [5] McGinnis D, Greinert J, Artemov Y, Beaubien SE, Wüest A. *Fate of rising methane bubbles in stratified waters: How much methane reaches the atmosphere?* *Journal of Geophysical Research* 2006;111(C09007): doi:10.1029/2005JC003183.
- [6] Schmale O, Greinert J, Rehder G. *Methane emission from high-intensity marine gas seeps in the Black Sea into the atmosphere*. *Geophysical Research Letters* 2005;32 (L07609):doi:10.1029/2004GL021138.
- [7] Dimitrov LI. *Mud volcanoes - a significant source of atmospheric methane*. *Geo-Marine Letters* 2003;23:155-161.
- [8] Leifer I, Patro RK. *The bubble mechanism for methane transport from the shallow sea bed to the surface: A review and sensitivity study*. *Continental Shelf Research* 2002;22:2409-2428.
- [9] Kessler JD, Reeburgh WS, Southon J, Seifert R, Michaelis W, Tyler SC. *Basin-wide estimates of the input of methane from seeps and clathrates to the Black Sea*. *Earth and Planetary Science Letters* 2006;243:366-375.
- [10] Reeburgh WS, Ward BB, Whalen SC, Sandbeck KA, Kilpatrick KA, Kerkhof LJ. *Black Sea methane geochemistry*. *Deep-Sea Research I* 1991;38(Supplement 2):S1189-S1210.
- [11] Jørgensen BB, Weber A, Zopfi J. *Sulfate reduction and anaerobic methane oxidation in Black Sea sediments*. *Deep-Sea Research I* 2001;48:2097-2120.
- [12] Reeburgh WS, Tyler SC, Carroll J. *Stable carbon and hydrogen isotope measurements on Black Sea water-column methane*. *Deep-Sea Research II* 2006;53:1893-1900.
- [13] Schubert CJ, Durisch-Kaiser E, Holzner CP, Klausner L, Wehrli B, Schmale O, Greinert J, McGinnis DF, DeBatist M, Kipfer R. *Methanotrophic microbial communities associated with bubble plumes above gas seeps in the Black Sea*. *Geochemistry, Geophysics, Geosystems* 2006;7(1): doi:10.1029/2005GC001049.

- [14] Wallmann K, Drews M, Aloisi G, Bohrmann G. *Methane discharge into the Black Sea and the global ocean via fluid flow through submarine mud volcanoes*. Earth and Planetary Science Letters 2006;248:544-559.
- [15] Klačucke I, Sahling H, Weinrebe W, Blinova V, Bürk D, Lursmanashvili N, Bohrmann G. *Acoustic investigation of cold seeps offshore Georgia, eastern Black Sea*. Marine Geology 2006;231:51-67.
- [16] Wagner-Friedrichs M, Bulgay E, Keil H, Krastel S, Bohrmann G, Ivanov M, Spiess V. *Gas seepage and gas/fluid migration associated with the canyon-ridge system offshore Batumi (Georgia, south-eastern Black Sea) inferred from multichannel seismic data*. International Journal of Earth Sciences submitted.
- [17] Michaelis W, Seifert R, Nauhaus K, Treude T, Thiel V, Blumenberg M, Knittel K, Gieseke A, Peterknecht K, Pape T, Boetius A, Amann R, Jørgensen BB, Widdel F, Peckmann J, Pimenov NV, Gulin MB. *Microbial reefs in the Black Sea fueled by anaerobic oxidation of methane*. Science 2002;297:1013-1015.
- [18] Naudts L, Greinert J, Artemov Y, Staelens P, Poort J, VanRensbergen P, DeBatist M. *Geological and morphological setting of 2778 methane seeps in the Dnepr paleo-delta, northwestern Black Sea*. Marine Geology 2006;227:177-199.
- [19] Aloisi G, Wallmann K, Haese RR, Saliège J-F. *Chemical, biological and hydrological controls on the ¹⁴C content of cold seep carbonate crusts: numerical modeling and implications for convection at cold seeps*. Chemical Geology 2004;213:359-383.
- [20] Heeschen KU, Hohnberg H-J, Haeckel M, Abegg F, Drews M, Bohrmann G. *In-situ hydrocarbon concentrations from pressurized cores in surface sediments, Northern Gulf of Mexico*. Marine Chemistry 2007;107(4):498-515.
- [21] Grasshoff K, Ehrhardt M, Kremling K. *Methods of Seawater Analysis*. Weinheim: Wiley-VCH, 1999.
- [22] Haeckel M. *A transport-reaction model of the hydrological systems of the Costa Rica subduction zone*. In: Klaus A, Morris J, Villinger H, editors. Proceedings of the Ocean Drilling Program, Scientific Results. College Station, TX: Ocean Drilling Program, 2006, p. 1-26.
- [23] Haeckel M, Suess E, Wallmann K, Rickert D. *Rising methane gas-bubbles form massive hydrate layers at the seafloor*. Geochimica et Cosmochimica Acta 2004;68(21):4335-4345.
- [24] Berner RA. *Early Diagenesis - A Theoretical Approach*. Princeton, New Jersey: Princeton University Press, 1980.
- [25] Li Y-H, Gregory S. *Diffusion of ions in sea water and in deep-sea sediments*. Geochimica et Cosmochimica Acta 1974;38:703-714.
- [26] Boudreau BP. *Diagenetic Models and Their Implementation: Modelling Transport and Reactions in Aquatic Sediments*. Berlin, Heidelberg, New York: Springer-Verlag, 1997.
- [27] Tishchenko P, Hensen C, Wallmann K, Wong CS. *Calculation of the stability and solubility of methane hydrate in seawater*. Chemical Geology 2005;219:37-52.
- [28] Jørgensen BB, Böttcher ME, Lüschen H, Neretin LN, Volkov II. *Anaerobic methane oxidation and a deep H₂S sink generate isotopically heavy sulfides in Black Sea sediments*. Geochimica et Cosmochimica Acta 2004;68(9):2095-2118.
- [29] Lu H, Matsumoto R. *Experimental studies on the possible influences of composition changes of pore water on the stability conditions of methane hydrate in marine sediments*. Marine Chemistry 2005;93:149-157.
- [30] Ussler W, Paull CK. *Ion exclusion associated with marine gas hydrate deposits*. In: Dillon WP, Paull CK, editors. Natural Gas Hydrates - Occurrence, Distribution, and Detection. Washington, DC: American Geophysical Union, 2001, p. 41-51.
- [31] Fofonoff NP, Millard RC. *Algorithms for computation of fundamental properties of seawater*. Unesco Technical Papers in Marine Science 1983;44:1-53.
- [32] Anderson AL, Abegg F, Hawkins JA, Duncan ME, Lyons AP. *Bubble populations and acoustic interaction with the gassy floor of Eckernförde Bay*. Continental Shelf Research 1998;18:1807-1838.
- [33] Chanton JP, Martens CS, Kelley CA. *Gas transport from methane-saturated, tidal freshwater and wetland sediments*. Limnology and Oceanography 1989;34(5):807-819.
- [34] Martens CS. *Control of methane sediment-water bubble transport by macroinfaunal irrigation in Cape Lookout Bight, North Carolina*. Science 1976;192:998-1000.

- [35] Martens CS, Albert DB, Alperin MJ. *Biogeochemical processes controlling methane in gassy coastal sediments - Part I. A model coupling organic matter flux to gas production, oxidation and transport*. Continental Shelf Research 1998;18:1741-1770.
- [36] Martens CS, Klump JV. *Biogeochemical cycling in an organic-rich coastal marine basin I. Methane sediment-water exchange processes*. Geochimica et Cosmochimica Acta 1980;44:471-490.
- [37] Reeburgh WS. *Observations of gases in Chesapeake Bay sediments*. Limnology and Oceanography 1969;14(3):368-375.
- [38] Boudreau BP, Algar C, Johnson BD, Croudace I, Reed A, Furukawa Y, Dorgan KM, Jumars PA, Grader AS, Gardiner BS. *Bubble growth and rise in soft sediments*. Geology 2005;33(6):517-520.
- [39] Johnson BD, Boudreau BP, Gardiner BS, Maas R. *Mechanical response of sediments to bubble growth*. Marine Geology 2002; 187:347-363.
- [40] Niewöhner C, Hensen C, Kasten S, Zabel M, Schulz HD. *Deep sulfate reduction completely mediated by anaerobic methane oxidation in sediments of the upwelling area off Namibia*. Geochimica et Cosmochimica Acta 1998; 62(3):455-464.
- [41] Schulz HD, Dahmke A, Schinzel U, Wallmann K, Zabel M. *Early diagenetic processes, fluxes, and reaction rates in sediments of the South Atlantic*. Geochimica et Cosmochimica Acta 1994;58(9):2041-2060.
- [42] Fossing H, Ferdelman TG, Berg P. *Sulfate reduction and methane oxidation in continental margin sediments influenced by irrigation (South-East Atlantic off Namibia)*. Geochimica et Cosmochimica Acta 2000;64(5):897-910.
- [43] Haeckel M, Wallmann K, Boudreau BP. *Bubble-induced porewater mixing: A 3-D model for deep porewater irrigation*. Geochimica et Cosmochimica Acta 2007;71(21):5135-5154.
- [44] Aller RC. *Quantifying solute distributions in the bioturbated zone of marine sediments by defining an average microenvironment*. Geochimica et Cosmochimica Acta 1980;44:1955-1965.
- [45] Aller RC, Aller JY. *Meiofauna and solute transport in marine muds*. Limnology and Oceanography 1992;37(5):1018-1033.
- [46] Meile C, Koretsky CM, VanCappellen P. *Quantifying bioirrigation in aquatic sediments: An inverse modeling approach*. Limnology and Oceanography 2001;46(1): 164-177.
- [47] Schlüter M, Sauter W, Hansen HP, Suess E. *Seasonal variations of bioirrigation in coastal sediments: Modelling of field data*. Geochimica et Cosmochimica Acta 2000; 64(5):821-834.
- [48] Davies RM, Taylor G. *The mechanics of large bubbles rising through extended liquids and through liquids in tubes*. Proceedings of the Royal Society of London. Series A 1950;200:375-390.
- [49] Prandtl L, Tietjens OG. *Fundamentals of Hydro- and Aerodynamics*: Dover Publications Inc., 1957.
- [50] Torres ME, Wallmann K, Trehu AM, Bohrmann G, Borowski WS, Tomaru H. *Gas hydrate growth, methane transport, and chloride enrichment at the southern summit of Hydrate Ridge, Cascadia margin off Oregon*. Earth and Planetary Science Letters 2004;226:225-241.
- [51] Torres ME, McManus J, Hammond DE, deAngelis MA, Heeschen KU, Colbert SL, Tryon MD, Brown KM, Suess E. *Fluid and chemical fluxes in and out of sediments hosting methane hydrate deposits on Hydrate Ridge, OR, I: Hydrological provinces*. Earth and Planetary Science Letters 2002;201:525-540.
- [52] Boles JR, Clark JF, Leifer I, Washburn L. *Temporal variation in natural methane seep rate due to tides, Coal Oil Point area, California*. Journal of Geophysical Research 2001;106(C11):27077-27086.